Inter-integration membrane-assisted reactive distillation for ethyl levulinate production: Equipment development and experimental validating

Wen-tao Han[1] | Zhen-wei Han[1] | Xue-chao Gao[2] | Zhou Hong[2] | Xin-gang Li[1] | Hong Li[1] | Xue-hong Gu[2,*] | Xin Gao[1,*]

[1]School of Chemical Engineering and Technology, National Engineering Research Center of Distillation Technology, Collaborative Innovation Center of Chemical Science and Engineering (Tianjin), Tianjin University, Tianjin 300072, China

[2]State Key Laboratory of Materials-Oriented Chemical Engineering, College of Chemical Engineering, Nanjing Tech University, Nanjing 211816, China

Corresponding authors: gaoxin@tju.edu.cn (X. Gao), xhgu@njtech.edu.cn (X.H. Gu)

Abstract: Ethyl levulinate, one of main derivatives of levulinic acid (LA), is of significant potential as platform chemicals for bio-based materials. The esterification of LA was generally carried out in a conventional batch reactor or in a conventional reactive distillation column. However, traditional methods are hard to deal with equilibrium limited reactions and azeotropic issues. Therefore, the reactive-vapor permeation-distillation (R-VP-D) process, which integrated reaction, distillation and membrane dehydration into one single unit, is proposed in this paper and validated in the pilot-scale experiments. A comparative study is made between a pilot-scale RD column with and without vapor permeation membrane module. Owing to the water-selective membrane and the ingenious design of related apparatuses, the R-VP-D process reveal a superiority in LA conversion of 21.9% maximum higher than RD without VP process and removing of product water about 53.6% from VP module, which indicates its promising
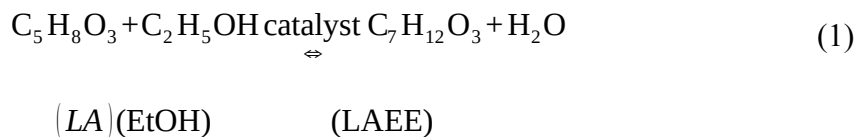
industrial application in process intensification field.

1 | INTRODUCTION

Ethyl levulinate (LAEE) is one of main derivatives of levulinic acid (LA), which has attracted considerable interest on account of its many advantages. For example, due to its high oxygen content (33 wt.%), it can be used as a next-generation fuel additive to improve the octane number of gasoline and reduce the CO and NO_X emissions.[1] LAEE is also used as a flavor additive in food industry and a fragrance additive in cosmetics.[2] Although the global LAEE industry is still in its nascent stage, LAEE has already attracted considerable attention and the global market is expected to reach $11.8 million by 2022. Esterification of ethanol (EtOH) and LA is one of the main methods for the production of LAEE, which was shown in Equation (1).[3] The esterification process of LA with EtOH is an equilibrium-limited reaction where the forward and backward reaction coexist, in addition, the reactant EtOH and the product water will form an azeotrope which will cause reaction inhibition and separation problem. Reactive distillation (RD) is one of the best known and most promising possibilities in increasing the yield of chemical equilibrium limited reactions and overcoming the formation of azeotropes,[4] it combines separation and reaction in a single unit, is a common application of process intensification.[5,6] Facilitating by the interaction of reaction and separation, RD has significant advantages in energy conservation, process simplification, selectivity improvement and purity enhancement.[7,8] These features are critical for the application of RD process in equilibrium limited reactions especially in esterification reactions.[9,10] To the best of our known, no experimental studies on LA esterification with RD technique has ever been reported, therefore, a RD process was proposed in

the synthesis of LAEE and a series of pilot-scale experiments were performed in this article to validate the feasibility of RD process.

$$C_5H_8O_3 + C_2H_5OH \underset{\Leftrightarrow}{catalyst} C_7H_{12}O_3 + H_2O \qquad (1)$$

$$\left(LA\right)(EtOH) \qquad (LAEE)$$

Pervaporation (PV) and vapor permeation (VP) are highly suitable in separating close boiling mixtures and overcoming azeotropes where RD is hard to reach or requires the use of an auxiliary agent.[11-13] Vapor permeation membrane is most suitable if the feed, retentate and permeate are all in a gaseous state, while the first two are on the high pressure side of the membrane, the remaining one is on the low pressure side.[14] Although the VP have been exclusively used in many industrial processes, the coupling of other separation units with the membrane provide an even more substantial benefits than conventional process, especially the combination of RD with VP.[15,16] Holtbruegge et al.[17] proposed a membrane-assisted reactive distillation process for the synthesis of dimethyl carbonate and propylene glycol, demonstrating the high potential of VP coupled with RD process. Novita et al.[18] investigated the reactive distillation with pervaporation hybrid configuration for enhanced ethyl levulinate production. They performed simulation studies for the production of LAEE with several different configurations, which demonstrated the advantage of RD process combined with pervaporation in lowering the cost and improving the energy efficiency. Steinigeweg and Gmehling[19] considered the transesterification of methyl acetate with n-butanol to produce butyl acetate and methanol. They conducted a simulation study for the membrane-assisted RD process and verify the feasibility of applying this process in terms of theory. However, these so called membrane-assisted RD processes all put the membrane outside the RD column, the redundant flow path between column and membrane separates the RD process from the membrane separation

3

process, the stand-alone operation of membrane unit is unable to achieve in situ product removal and hard to influence the reaction progress in RD column. The reactive-vapor permeation-distillation (R-VP-D) process, which integrates vapor permeation and reactive distillation into one unit, is proposed in this work to solve the difficulties that are hard to fix by RD-VP/PV processes. For the LA esterification, the in situ removal of water from the reaction zone by VP unit directly promotes the forward progress of the reversible reaction and increases the yield of desired product, and azeotrope of EtOH and water can be overcome as the water is removed. Compared to RD-VP/PV processes, the R-VP-D process has a reduced number of apparatuses, a lower investment and operating cost saving on account of all of these advantages. However, the design of R-VP-D column is challenging due to the high integration degree and the unmanageable liquid phase in the membrane separated section (MSS). The design of the membrane module coupled inside the column (MMIC) is also a problem as the membrane was in a semi-close state in the RD column, which means the membrane needs to be in good contact with the gas phase inside the column without causing short cut of the gas. Therefore, experimental investigations at pilot scale are crucial to verify the feasibility of R-VP-D process and self-designed R-VP-D column.

In this paper, the R-VP-D process, an evolutional hybrid process embedding vapor permeation unit inside the reactive distillation process, is proposed for the azeotrope overcoming and the reaction promoting of LA esterification. A hollow fiber NaA zeolite membrane module with excellent separation performance was adopted for in-situ dehydration of reactive mixture. Several self-designed devices including MMIC, MSS and R-VP-D column are used and validated in this work. A series of pilot-scale R-VP-D experiments, RD experiments and reactive distillation without vapor permeation (R-W-V) experiments have been performed to verify the

feasibility of the R-VP-D process, and comparisons were conducted among these three processes.

2 | EXPERIMENTAL INVESTIGATION

2.1 | Materials

EtOH (99.9 wt.%) was obtained from Tianjin Rionlon Chemical and Medical Co., Ltd, and levulinic acid (99.0 wt.%) was supplied by Shanghai Macklin Biochemical Co., Ltd. The internal standard, Ethyl laurate (99.0 wt.%), used for gas chromatography analysis, was supplied by Shanghai 9ding Biological Technology Co., Ltd. Ethyl levulinate (99.0 wt.%) was also supplied by Shanghai 9ding Biological Technology Co., Ltd. The heterogeneous catalyst, acidic exchange resins KRD-001, was supplied by Kairui Environmental Protection Technology Co., Ltd. The hollow fiber NaA zeolite membrane modules (HFZM) were fabricated by Nanjing Tech University.[20] The modules were prepared by an ensemble synthesis strategy, which has been reported previously.[21]

2.2 | Analysis

2.2.1 | Gas chromatograph

Analysis of the samples in this work was performed using a Gas Chromatography (GC) (Chemito 8610) with a flame-ionization detector. A 30 m long Agilent HP-INNOWAX supplied by Agilent Technology was adopted. Each sample was analyzed at least three times with the averaged data to identify possible statistical errors of the GC analysis.
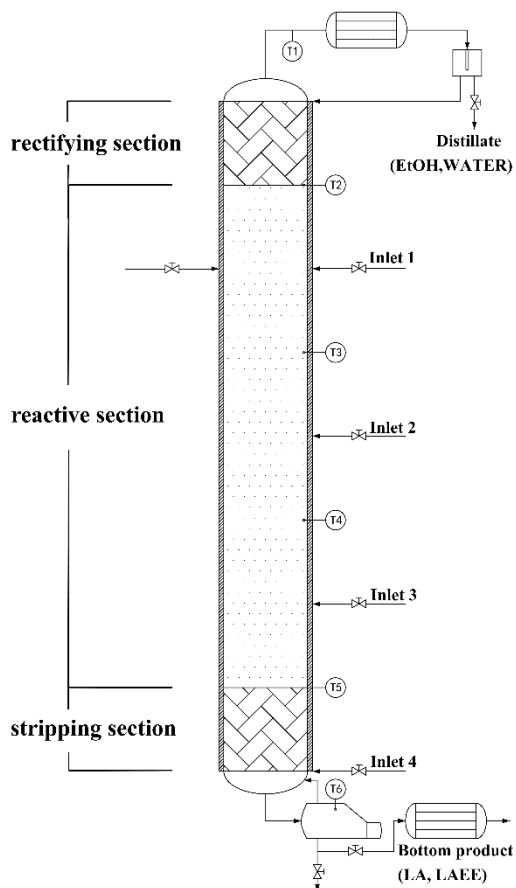
2.1.2 | Karl Fisher moisture titration

The content of water in samples were measured by Karl Fischer moisture titration. Karl

Fischer titration was a classic titration method in chemical analysis, which was selective for water with a high accuracy and precision, typically within 1% of available water.

2.3 | Conventional reactive distillation experiments

2.3.1 | The RD column setup
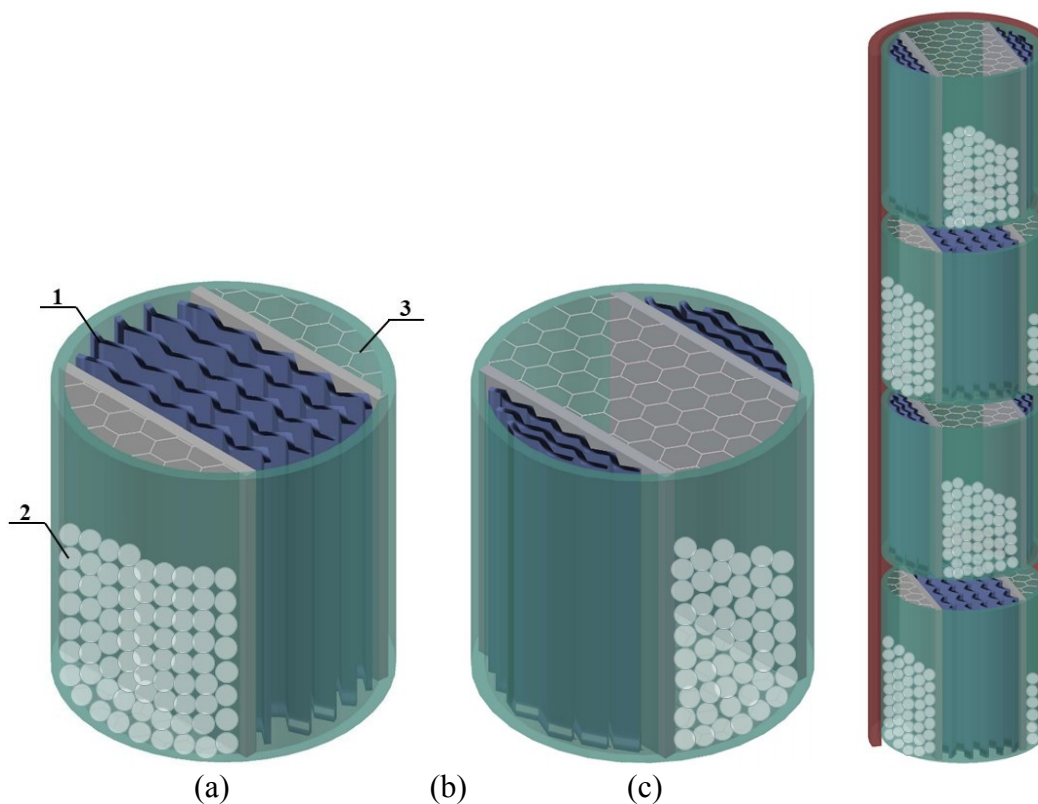

FIGURE 1 Continuous RD set-up

A series of pilot-scale experiments for the synthesis of LAEE from LA and EtOH had been carried out in a pilot plant reactive distillation column with SCPIs. Figure 1 showed the schematic of the continuous RD column used in this part. The column was made of stainless steel with the internal diameter of 50 mm and an overall height of approximately 3500 mm. The total

packing height of the pilot-scale column was 2000 mm, it consisted of three sections: the rectifying and the stripping sections with each 250 mm long, and the middle reactive section with a length of 1500 mm. The striping section and the rectifying section were filled with θ-ring packings, while the reactive section contained θ-ring packings and Seepage Catalytic Packing Internals (SCPIs). An electric jacket was wrapped around the column to reduce heat loss and eliminate the impact of environmental factor. As we could see in the Figure 1, the reboiler was a vessel at the bottom of the column, the external oil bath was responsible for regulating its temperature. WRNK-171 (accuracy of ±0.1°C) Thermometers were installed evenly into the column and the reboiler to collect temperature information. The majority gas phase of this chemical system was mainly EtOH and water, it was condensed by a condenser as it raised to the top of the RD column, the cold water at 15°C was used as the cooling medium. Electronic balance (accuracy of ±0.01 kg) was used to record weight changes of the input streams and the output streams. Liquid sampling point was located at the bottom of the column and light sampling point was at the top, the gas chromatography was used to analyze the samples after they were been cooled down. A LPC control system was run on the window 7 as the control center to regulate and record the column temperature and the weight changes of electronic balance, the other functions of LPC control system were to observe the data changes of RD column and to control the reflux ratio (RR) controller.

2.3.2 | Seepage Catalytic Packing Internals

In this work, the Seepage Catalytic Packing Internals (SCPIs), developed by the National Engineering Research Center for Distillation Technology in China, was loaded in the reactive section of the pilot-scale RD column. As shown in Figure 2, it was composed of two segments, one had the catalysts in the middle and the packings on both sides like Figure 2a, and the other

was the opposite like Figure 2b. These two segments were arranged crosswise and worked together like Figure 2c. The external diameter of SCPIs was 50 mm, the same as the internal diameter of the pilot-scale RD column, and each segment of SCPIs had a height of 50 mm. Our previous study revealed its higher operational capacity and lower pressure drop than conventional column internals for heterogeneous catalyst distillation. The main description of SCPIs parameters could be found in our previous work.[22-24]

FIGURE 2 Graphic model of two segments of SCPIs and their installation status in the column. 1: packing, 2: catalyst, 3: wire mash. (a) left segment of SCPIs, (b) right segment of SCPIs, (c) installation status of SCPIs

The acidic ion exchange resins KRD-001 were chosen as the catalyst, which was immobilized in the catalyst filling area of the SCPIs. As shown in Figure 2a and b, the wire mesh was installed on the top and at the bottom of the catalyst filling area to encapsulate the catalyst, while 20 ml θ-ring packing was loaded between every two segments to promote the gas-liquid

mass transfer.

2.3.3 | Experimental procedure

The process of RD experiment was as follows: (1) Washing tower to eliminate impurities and the effects of residual substances from the previous experiment. (2) Start-up by adding raw materials to the reboiler to establish the total reflux. (3) Feeding EtOH and LA continuously by peristaltic pumps, the peristaltic pump needed to be calibrated in advance to meet the expected value. (4) At the end of the whole process, stop feeding and turn off the reboiler heating.

Start-up was the most crucial step in RD experiment. In order to achieve steady state as soon as possible, the experiment run was initialed by charging the reboiler with 155 g EtOH and 155 g LA (feed mole ratio (FMR) (EtOH/LA) was about 2.5:1). Total reflux was established in about 2 hours and another 2 hours were taken to meet the stable operation. After this, the raw material EtOH and LA were continuously fed, which meant the experiment had the officially started.

There were three variables that needed to be adjusted throughout the process: RR, FMR and feeding position. Every times before one condition was done and another round of testing was conducted, the following three criteria needed to be met:

(1) The mass sum of the input was equal to the mass sum of the output.

(2) The temperature at each temperature measurement points remained unchanged for a certain period of time.

(3) The composition of the samples remained unchanged for a period of time.

As these three conditions were met, this steady state was maintained for another 2 hours in order to withdraw samples, four sets of samples were withdrawal from the top and the bottom of RD column, these samples were then analyzed by GC as the final results.

2.3.4 | Design of experiments

In this part, three parameters were investigated and eight experiments were performed. The whole experimental process could be divided into three parts. Exp 1 to Exp 3 examined the effect of the RR, Exp 3 to Exp 6 examined the effect of feeding position, Exp 7 and Exp 8 with Exp 3 could obtain the effect of FMR in the experiment.

TABLE 1 Average mass flow rates and operating conditions of eight experiments performed in the pilot-scale column

	LA (g h^{-1})	EtOH (g h^{-1})	RR	FMR (EtOH/LA) (mol mol^{-1})	Inlet point of EtOH	Distillate (g h^{-1})	Bottom (g h^{-1})
Exp 1	153.5	155.8	1.00	2.558	Inlet4	127.2	182.1
Exp 2	155	154.2	2.00	2.508	Inlet4	136.6	172.6
Exp 3	156.5	153.6	0.50	2.474	Inlet4	126.8	183.3
Exp 4	154.5	155.2	0.50	2.532	Inlet3	127.5	182.2
Exp 5	155.3	156.2	0.50	2.535	Inlet2	137.2	174.3
Exp 6	155	153.1	0.50	2.490	Inlet1	137.3	170.8
Exp 7	157	92.4	0.50	1.483	Inlet4	73.7	176.1
Exp 8	103.5	143	0.50	3.482	Inlet4	117.1	129.4

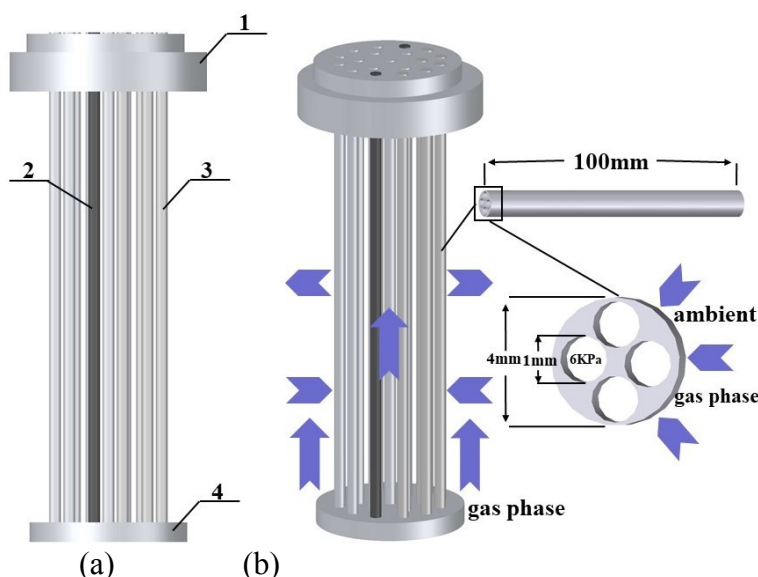Abbreviations: LA, levulinic acid; RR, reflux ratio.

Table S1 showed the starting, sampling and ending time of eight experiments, average mass flow rates and operating conditions of these eight experiments were summarized in Table 1. For example, as shown in Tables 1 and S1, at the 53.5th hour, the feeding position of EtOH was turned to Inlet Point 2 to conduct Exp 5, and the sampling time for Exp 5 was from the 61th hour to the 63th hour. The samples collected within the most stable state for each experiment

(illustrated in shaded area) were selected for analyzation.

2.4 | R-VP-D experiments

2.4.1 | Experimental setup

2.4.1.1 | Hollow fiber zeolite membrane module

FIGURE 3 Graphic model of HFZM and the cross section view of NaA zeolite membrane. 1: ceramic porous cover, 2: support rod, 3: hollow fiber NaA zeolite membrane tube, 4: ceramic base. (a) front view of HFZM, (b) graphic model of HFZM and NaA zeolite membrane
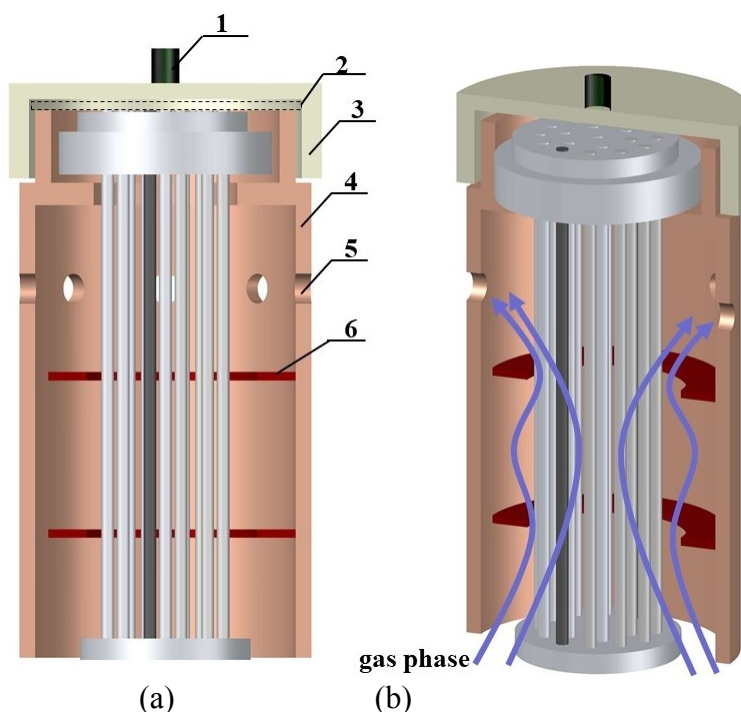
The hollow fiber supported NaA zeolite membrane module (HFZM), consisted of ceramic porous cover, ceramic base, support rod and a bundle of hollow fiber tubes, was prepared on the basis of NaA zeolite membranes. As shown in Figure 3, the NaA membranes were synthesized on four-channel ceramic support, which had an external diameter of 4 mm, and each channel had an internal diameter of 1 mm. The hollow fiber supported NaA zeolite membranes were considerably superior in permeation flux and mechanical strength.

There were 17 hollow fiber membranes used for dehydration and 2 ceramic rods used for supporting in the HFZM.[25,26] The open end of the membranes were fixed onto the porous cover,

11

while the other end were capped with ceramic base. The porous cover was then used for the formation of vacuum chamber.[27]

As shown in Figure 3, the NaA zeolite membranes, with strong hydrophilicity and an effective pore size of 0.42 nm, was highly selective for permeating water preferentially with a relatively high permeation flux. It made use of the difference of the adsorption and diffusion rate between the components to achieve the high purity, so the separation performance was unlimited by the thermodynamic equilibrium between the components. In water/EtOH mixture, a high separation factor was observed in vapor permeation through the NaA membrane.[28]

2.4.1.2 | Membrane module coupled inside the column

(a)   (b)

FIGURE 4 Graphic model of self-designed MMIC and the gas flow path in MMIC. 1: vacuum port, 2: vacuum chamber, 3: vacuum seal head, 4: annular seal base, 5: gas phase outlet, 6: annular baffle. (a) front view of MMIC, (b) graphic model of MMIC and the gas flow path

The self-designed membrane module coupled inside the column (MMIC) was a membrane separated device composed of HFZM and an external shell structure that could connected with

12

the RD column. The external shell structure consisted of the vacuum seal head, annular seal base, gas phase outlet, vacuum port and annular baffle. The vacuum seal head and the annular seal base were connected together through thread to make the area of porous cover a vacuum chamber. The undersurface of annular seal base was open wide to receive the rising gas phase, and a number of annular baffles were set to optimize the flow direction, which ensured the fluid to flow throughout the entire module, and it could also help each fiber contact with the flow, so that the gas shortcut could be avoided. The gas phase outlets, which have a total flow area of 7.85 cm^2, ensured that the gas could be discharged from the MMIC, thereby ensuring continuous of the gas phase. The vacuum port was connected to a vacuum line for the process of VP.
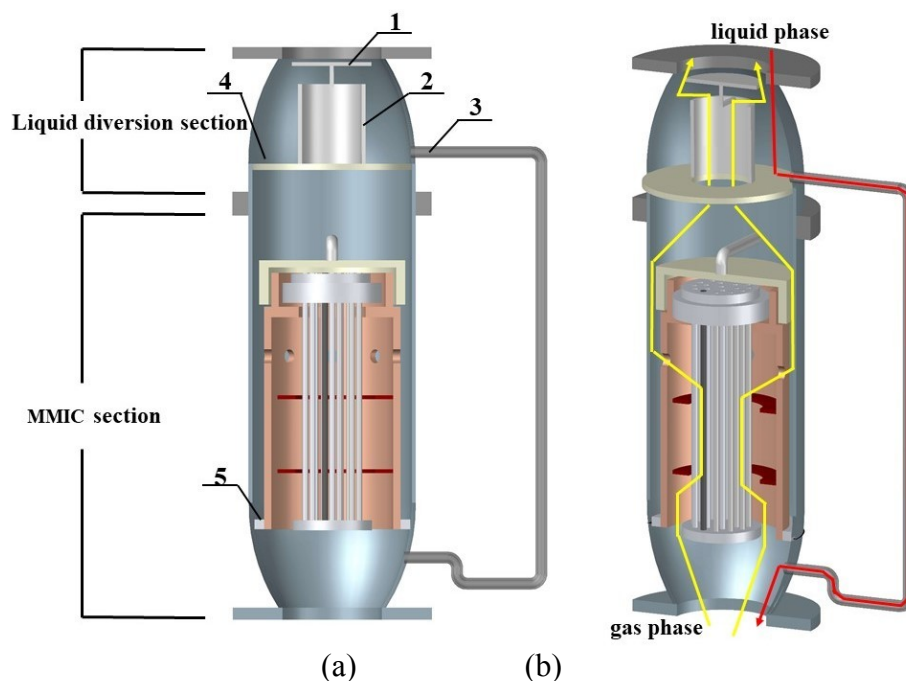
Different from the conventional membrane modules connected outside the column, the MMIC was coupled inside the column, and the ingenious design of MMIC integrated RD column and itself into a single unit. The process of gas phase flowing through MMIC was summarized as follows: As given in Figure 4b, the rising gas phase flowed into the MMIC, after the baffle action, each fiber had a full contacting with the flow, and it finally got outside from the MMIC through the gas phase outlet.

2.4.1.3 | Membrane separated section

The self-designed membrane separated section (MSS) was mainly composed of two parts, the upper was liquid diversion section and the lower was MMIC section. In order to investigate the effect of VP on the process of reactive distillation and to eliminate the interference of liquid phase to VP process, a liquid diversion section was set to separate the liquid phase from the gas phase. It was composed of effusion tray, ventilation dust, liquid cover plate and draft tube. The ventilation dust allowed the passage of rising gas phase, while the liquid cover plate blocked the falling liquid phase, and the effusion pan together with the draft tube was the only access to

guide liquid phase.

The MMIC section was shown in Figures 4 and 5, the vacuum port of MMIC extended to the vacuum-pumping system outside the R-VP-D column through pipeline, and a ring gasket was set at the bottom of the MMIC to expand its external diameter, in other words, the ring gasket played a role in closing the gap between the MMIC and outer column, and it also had a supporting effect for MMIC.
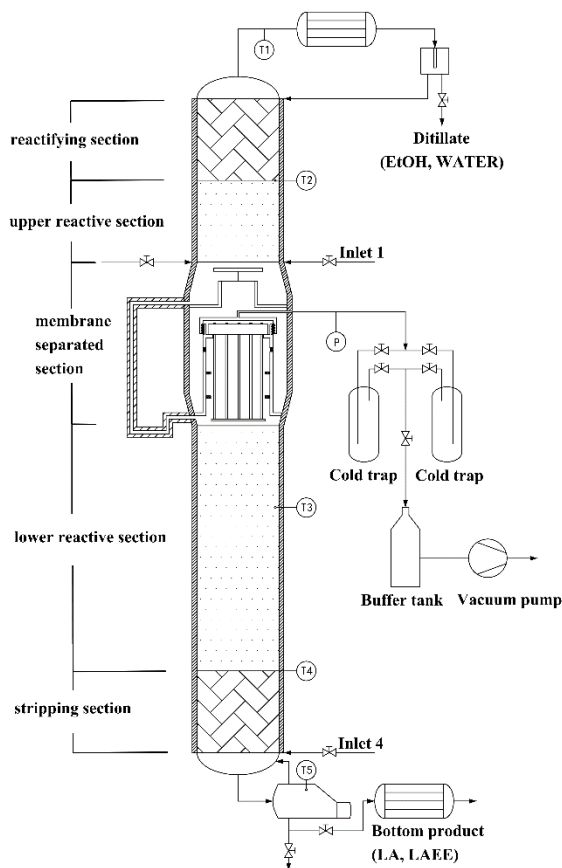

(a)   (b)

FIGURE 5 Graphic model of self-designed MSS and the gas flow path and liquid flow path in MSS. 1: liquid cover plate, 2: ventilation dust, 3: draft tube, 4: effusion tray, 5: ring gasket. (a) front view of MSS, (b) graphic model of MSS and flow path of gas and liquid

As the rising gas phase got into the MMIC section, due to the closure effect of the ring gasket and the full opening undersurface of the MMIC, the gas phase almost completely entered into MMIC and got outside through gas phase outlet and then rose into the liquid diversion section, the setup of the ventilation dust allowed the gas phase rising without barriers and got into the upper column section smoothly.

Due to the hindering effect of the liquid cover plate, the liquid phase flowed from above

gathered on the effusion tray and it was then diverted along the draft tube to the bottom of MSS. The gas-liquid separation mode of the MSS, which ingeniously avoided the interference of liquid to VP unit, was an effective and important link in the process of R-VP-D.

2.4.1.4 | The R-VP-D column setup

FIGURE 6 Self-designed R-VP-D column set-up

The R-VP-D column was modified from the conventional RD column by embedding a VP unit between two reactive sections, as shown in Figure 6, a sequence of reaction-vapor permeation-reaction was formed in the R-VP-D column, it was quite different from the usual RD-PV or RD-VP process, due to the in situ product removal and azeotrope overcoming effect, the R-VP-D column had a considerable advantage than conventional RD column. The self-

designed R-VP-D column had a total height of 3500 mm, the same height as RD column. Owing to the existence of MSS, the column was divided into five parts: the rectifying section, the upper reactive section, the membrane separated section, the lower reactive section, the stripping section, their lengths were 250 mm, 250 mm, 500 mm, 750 mm and 250 mm, respectively. The rectifying section and the stripping section were filled with θ-ring packings (3×3 mm), the upper reactive section and the lower reactive section were filled with θ-ring packings and SCPIs, while not any θ-ring packing or SCPIs was added into the membrane separated section. To maintain a stable operating temperature of the column, the column outside wall and the liquid draft tube were surrounded by an insulation jacket with a layer of mineral wool and an electric heating wire. The vacuum port of MMIC was connected to the vacuum pump outside the column through the pipeline. Two cold traps under liquid nitrogen cooling and working alternatively were installed between the MMIC and the vacuum pump to condense the gas phase extracted during the pilot-scale R-VP-D experiments.

2.4.2 | Experimental procedure

The pilot-scale R-VP-D experimental procedure had very few differences from the conventional RD experiment. In the start-up step, after the process of total reflux, the vacuum pump started and the permeate was extracted from the lumens of the hollow fibers. The permeate pressure was maintained at a pressure below 6 kPa. In the R-VP-D process, there were three variables that needed to be adjusted: RR, FMR and feeding position, which were the same as RD process.

2.4.3 | Design of experiments

Six experiments (numbered as Exptl 1-Exptl 6) were performed and the operating

16

parameters, such as RR, FMR of the reactants and the feeding position of EtOH were analyzed. Furthermore, to identify the impact of VP on the performance of RD process, another three experiments (numbered as Exptl 7-Exptl 9) were performed with the vacuum pump turned off. These three experiments were called collectively as RD without VP (R-W-V) process as the membrane was not activated when the pump turned off. The R-W-V process was actually a normal RD process but a better comparison with the R-VP-D process as these two processes were almost the same except for the lack of VP in the R-W-V process.

TABLE 2 Average mass flow rates and operating conditions of nine experiments performed in the pilot-scale column

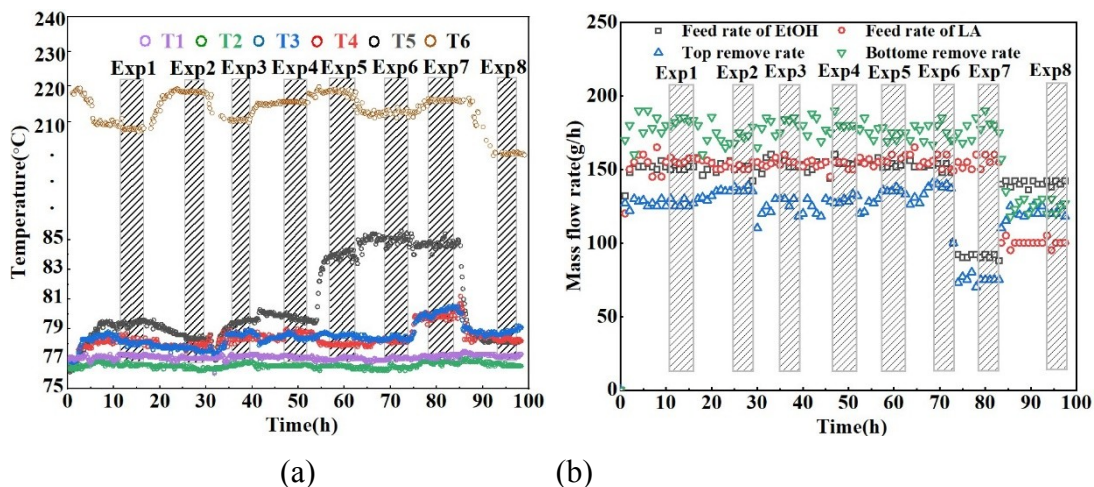|	Exptl 1	Exptl 2	Exptl 3	Exptl 4	Exptl 5	Exptl 6	Exptl 7	Exptl 8	Exptl 9
Vacuum	on	on	on	on	on	on	off	off	off
LA (g h^{-1})	128.5	128.5	128.5	128.5	128.5	103.5	128.5	128.5	103.5
EtOH (g h^{-1})	127.5	127.5	127.5	127.5	76.5	143	127.5	127.5	143
Permeate (kPa)	7.10	6.90	6.90	6.90	6.90	7.00	——	——	——
RR	0.5	1	2	0.5	0.5	0.5	0.5	2	0.5
FMR (mol mol^{-1})	2.5	2.5	2.5	2.5	1.5	3.5	2.5	2.5	3.5
EtOH Inlet	Inlet4	Inlet4	Inlet4	Inlet1	Inlet4	Inlet4	Inlet4	Inlet4	Inlet4
Distillate (g h^{-1})	101.5	102	102.3	98.6	49.7	125.6	100	100	125
Bottom (g h^{-1})	148.8	147.9	146.2	153.1	152.2	114.1	156	156	121.5
Permeate (g h^{-1})	5.7	6.1	7.5	4.3	3.1	6.8	——	——	——

Abbreviations: LA, levulinic acid; RR, reflux ratio.

The beginning of feeding was set to 0th hour in this part. Table S2 showed the starting,

sampling and ending time of Exptl 1 to Exptl 6 in R-VP-D process. For example, the FMR was reset to 3.5 at the 66.5th hour to perform Exptl 6. At the 78.5th hour, steady state was achieved, and sampling was performed. After the sample performed of Exptl 6, the vacuum pump turned off and the time was set to 0th for a better distinction with experiments before. Table S3 showed the starting, sampling and ending time of Exptl 7 to Exptl 9 in R-W-V process, and average mass flow rates and operating conditions of these nine experiments were summarized in Table 2.

3 | RESULTS AND DISCUSSIONS ON CONVENTIONAL RD

3.1 | Experimental results

(a)   (b)

FIGURE 7 Experimental data of Exp 1-Exp 8: (a) temperature of T1-T6, (b) feed and withdraw rates

In this part, there were three goals needed to be achieved: (1) Validate the feasibility of the production of LAEE with the aid of RD. (2) Investigate the impact of relevant parameters. (3) Prepare for the reactive-vapor permeation-distillation experiments.

Within the experimental investigation, 8 pilot-scale experiments were successfully performed in order to evaluate the effect of RR, FMR and feed-in-stage on the performance of

RD synthesis. Figure 7 showed the temperature profile of RD column and mass flow rate of feed and products in the experimental running process. The shaded area in Figure 7 indicated the steady state under these experiments, all experiment had been running for more than 10 hours to reach the steady state operating conditions, while the sampling times in the last two hours were 4 to get the error analysis. Fluctuations were observed in the data collected at temperature sampling points in Figure 7, especially the temperature detected in the temperature sampling point two (T2), it was due to the location of T2 was close to the in-flow point of the reflux stream. Experimental results were given in Table 3, for example, as can be seen in Exp 3, LA conversion of 60.1% in combination with LAEE purity of 62.87 wt.% was achieved.

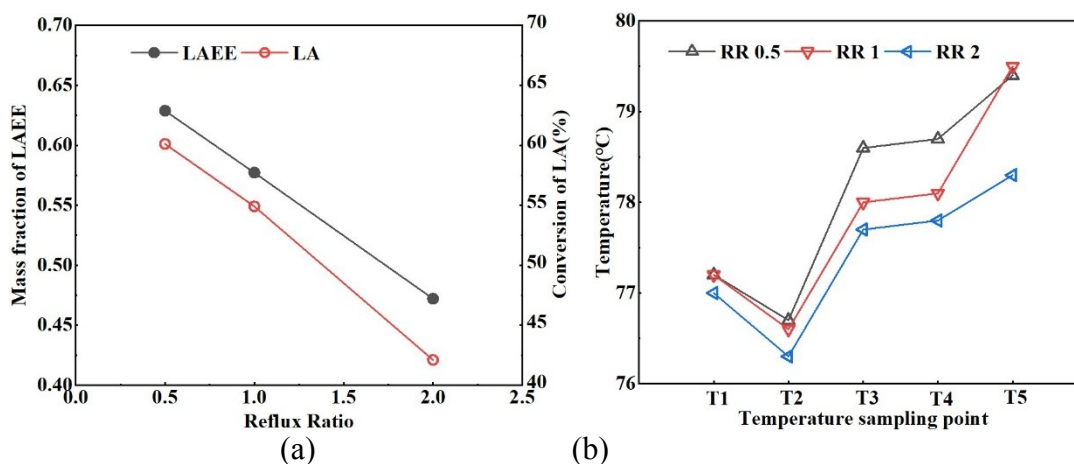**TABLE 3** Experimental results of eight steady periods for RD process

		Exp 1	Exp 2	Exp 3	Exp 4	Exp 5	Exp 6	Exp 7	Exp 8
Composition of top products (wt. %)	LA	trace	trace	trace	trace	trace	trace	trace	trace
	EtOH	91.609	94.139	90.392	91.460	93.198	94.669	90.413	92.192
	LAEE	trace	trace	trace	trace	trace	trace	trace	trace
	Water	8.931	5.861	9.608	8.540	6.802	5.331	9.587	7.808
Composition of bottom products (wt. %)	LA	41.818	51.946	36.187	44.730	54.626	55.942	50.134	30.041
	EtOH	0.741	0.802	0.943	0.905	0.635	0.781	0.608	1.251
	LAEE	57.710	46.610	62.870	53.890	44.160	42.470	48.510	68.350
	Water	0.472	0.642	0.850	0.475	0.579	0.807	0.748	0.358

| LA conversion | 0.549 | 0.421 | 0.601 | 0.511 | 0.397 | 0.381 | 0.438 | 0.646 |

Abbreviations: LA, levulinic acid; LAEE, ethyl levulinate; RD, reactive distillation.

3.2 | Effect of RR

RR, an important parameter for the RD process, was defined as ratio of reflux given to the column to the reflux sent to the distillate. As shown in Figure 8, an investigation of RR ranged from 0.5 to 2 had been conducted with other operating conditions kept unchanged. LA conversion dropped significantly from 0.601 to 0.421 along with the RR increasing from 0.5 to 2, while the mass fraction of LAEE decreased from 0.629 to 0.466.

(a) (b)

FIGURE 8 Effects of RR on purity of LAEE and conversion of LA and temperature profile: (a) mass fraction of LAEE and conversion of LA, (b) temperature of different temperature sampling points. (Experimental conditions: FMR (EtOH/LA): 2.5, total feed rate 310 g/h, LA feeding location: Inlet point 1, EtOH feeding location: Inlet point 4, D/F: 0.41, 1 atm)

The results revealed a completely different trend from the usual changes in RR to conversion of RD process. By increasing the RR, a larger reflux stream rich in EtOH entered the RD column, resulting in a higher EtOH concentration and increased internal flow rates in the reactive section of RD column. The heterogeneous acid catalyst immobilized in the SCPIs, which had the same concentration referred to the feed mass flow rate for both reactants, was thus

diluted at a higher RR, resulting in a lowered reaction rate, and a higher internal flow rates would also result in a shortened residence time of LA in the reactive section. In addition, as RR increased, owing to the existence of an azeotrope consist of EtOH and water, product water was difficult to be distilled and separated in time so that it hindered the reaction progress in the forward direction. Under a multiple effect on the reaction rate, the increased EtOH concentration in the reactive reaction was compensated by the catalyst dilution and azeotropic effect, therefore, the purity of LAEE and the conversion of LA decreased along with the increase of RR.
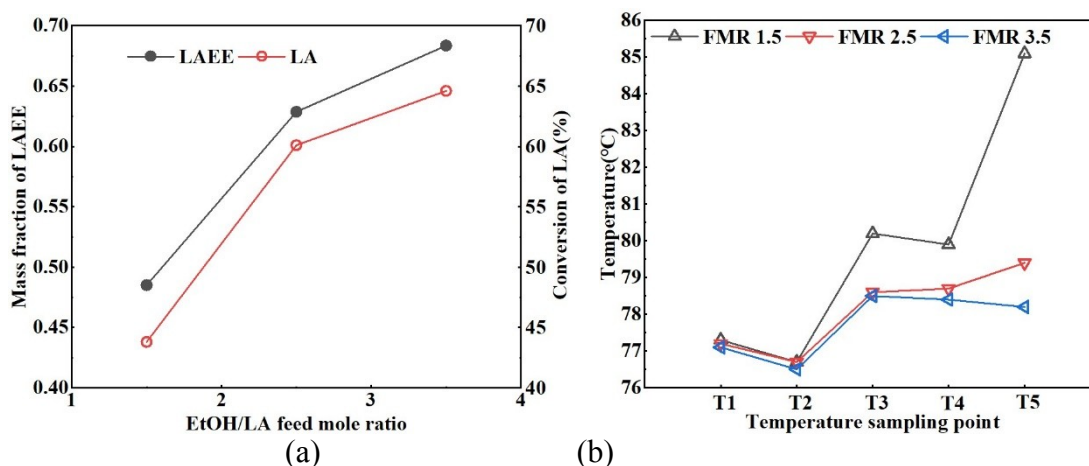
As shown in Figure 8b, the discussed effect of the RR on the purity of LAEE and conversion of LA was also identified by the temperature profile of RD column. By increasing the RR, the temperatures of T3 and T4 which directly measured the temperature variation of reactive section decreased. It was caused by a lowered reaction rate of LA esterification in the reactive section which led to a higher EtOH concentration in the RD column. As the EtOH was the lightest component in this chemical system, a higher EtOH concentration would significantly bright down the temperature of the RD column.

3.3 | Effect of FMR

An excessive EtOH could enhance the conversion of LA, the FMR (EtOH/LA) of 1.5, 2.5 and 3.5 were investigated in the pilot-scale experiments with other operating conditions unchanged. Due to a limited capacity of the RD column, the feeding rate of LA was kept unchanged at about 155 g/h in Exp 3 and Exp 7, 103.5 g/h in Exp 8, while the feeding rate of EtOH was 92.4 g/h, 153.6 g/h and 143 g/h, respectively. As shown in Figure 9a, with the increase of FMR from 1.5 to 3.5, the conversion of LA increased significantly from 0.438 to 0.646 and the purity of LAEE increased from 0.485 to 0.684. With an increase of FMR, the mass fraction of LA was lowered in the column as more EtOH was introduced into the column. As we know,

increasing one reactant would lead to a better conversion of other reactants, therefore, the conversion of LA increased with the rise of FMR. As EtOH was the lightest component in this chemical system, the majority of EtOH rose to the top of column, therefore, the mass fraction of LAEE at the bottom of column also increased because there was almost no diluting effect in the bottom of column caused by excessive EtOH.

The temperature profile was also affected by an increased FMR in the investigated operating range of the pilot-scale column. As shown in Figure 9b, the temperature of T1 to T5 dropped as the FMR was higher, it was due to the raised presence of EtOH at a higher FMR, which gave a cooling effect to the RD column.

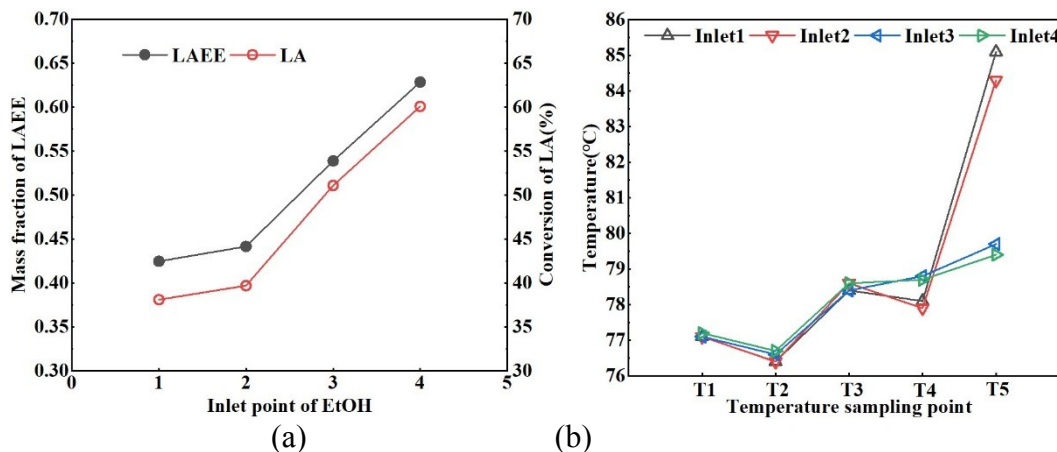(a)   (b)

FIGURE 9 Effects of FMR on purity of LAEE and conversion of LA: (a) mass fraction of LAEE and conversion of LA, (b) temperature of different temperature sampling points. (Experimental conditions: RR: 0.5, LA feeding location: Inlet point 1, EtOH feeding location: Inlet point 4, 1 atm)

3.4 | Effect of position of feeding

Different feeding positions were investigated with other operating conditions unchanged. It was undoubted that the feed-in position of the light reactant needed to be lower than heavy reactant. In this investigation, since LA was nearly non-volatile in the RD column, the feeding position of LA was fixed, while the feeding position of EtOH was varied from inlet point 1 to

inlet point 4 to investigate the effect of feed-in location on the experimental results. As shown in Figure 10a, the LA conversion increased slightly from 0.381 to 0.397 as the feeding position of EtOH changed from inlet point 1 to inlet point 2, and the conversion of LA up to 0.601 could be obtained at inlet point 4. Significant increments of LAEE purity and LA conversion were observed at inlet point 3 and 4.

(a)   (b)

FIGURE 10 Effects of EtOH feeding location on purity of LAEE and conversion of LA: (a) mass fraction of LAEE and conversion of LA, (b) temperature of different temperature sampling points. (Experimental conditions: RR: 0.5, FMR (EtOH/LA): 2.5, total feed rate: 310 g/h, LA feeding location: Inlet point 1, D/F:0.40, 1 atm)
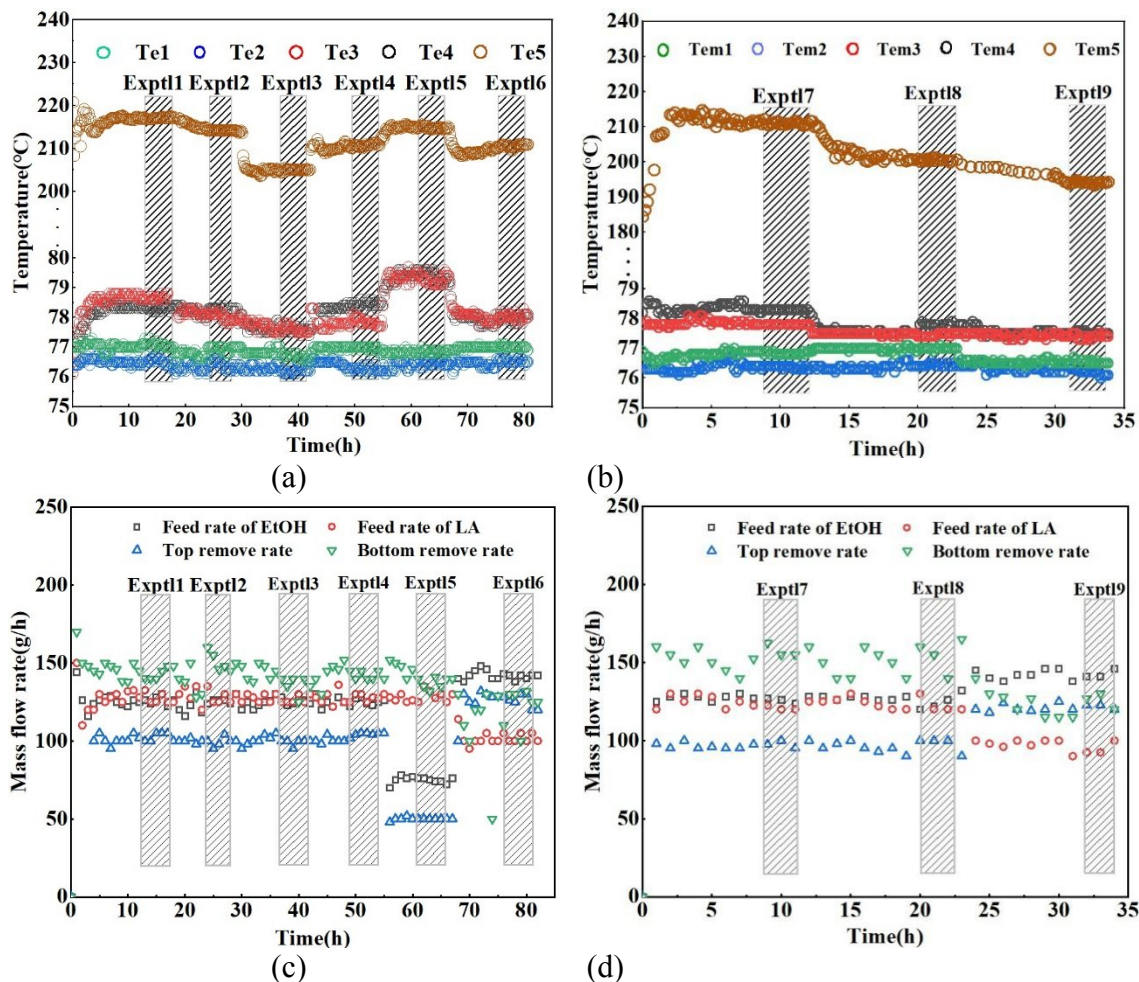
As shown in Figure 10a and b, the feeding position had a significant influence in concentration profile and temperature profile. As the normal boiling point of EtOH (78°C) was quite different from that of LA (245°C), the optimal feed location was relatively obvious in this series of experiments. Due to the increased contact time of EtOH and LA, inlet point 4 for EtOH facilitated the conversion of LA as well as the purity of LAEE.

4 | RESULTS AND DISCUSSIONS ON R-VP-D PROCESS

4.1 | Experimental results

The experimental investigation in this part was to verify the feasibility of R-VP-D process

and to compare the results with R-W-V experiments and previous RD experiments, in addition,

feasibility and availability of the self-designed R-VP-D column also needed to be verified.

(a)

(b)

(c)

(d)

FIGURE 11 Experimental data of Exptl 1-Exptl 9: (a) temperature profile of R-VP-D process,
(b) temperature profile of R-W-V process, (c) feed and withdraw rates of R-VP-D process, (d)
feed and withdraw rates of R-W-V process

As shown in Table 4, within the experimental investigation of R-VP-D process and R-W-V

process, nine pilot-scale experiments were successfully conducted with the effect of RR, FMR

and feeding position evaluated. Figure 11 showed the temperature profile and the change of mass

flow rate of R-VP-D process and R-W-V process. The shaded area in Figure 11 indicated the

steady state. As shown in the temperature profile of Figure 11a, the temperature of R-VP-D

column uniformly distributed from 76°C to 80°C. As shown in the feed and withdraw flow rate of Figure 11c and 11d, the flow rate of incoming and outgoing materials remain stable, and mass was conserved in the whole process. Available from the experimental results, the water content of the permeate was all above 99.0 wt.%, indicating that the VP unit worked normally in the whole process.

TABLE 4 Experimental results of R-VP-D process and R-W-V process

	Composition of top (wt.%)				Composition of bottom (wt.%)				LA conversion
	LA	EtOH	LAEE	water	LA	EtOH	LAEE	water	
Exptl 1	trace	97.329	trace	2.671	40.356	0.683	58.681	0.280	0.544
Exptl 2	trace	97.507	trace	2.493	38.925	0.771	59.793	0.511	0.555
Exptl 3	trace	97.224	trace	2.776	34.261	0.723	64.712	0.304	0.600
Exptl 4	trace	97.650	trace	2.350	51.147	0.819	47.710	0.324	0.443
Exptl 5	trace	97.483	trace	2.517	44.205	0.630	54.665	0.500	0.521
Exptl 6	trace	96.717	trace	3.283	36.474	1.110	61.991	0.425	0.550
Exptl 7	trace	93.384	trace	6.616	50.770	0.730	47.492	1.008	0.464
Exptl 8	trace	93.870	trace	6.130	59.009	0.825	38.920	1.246	0.381

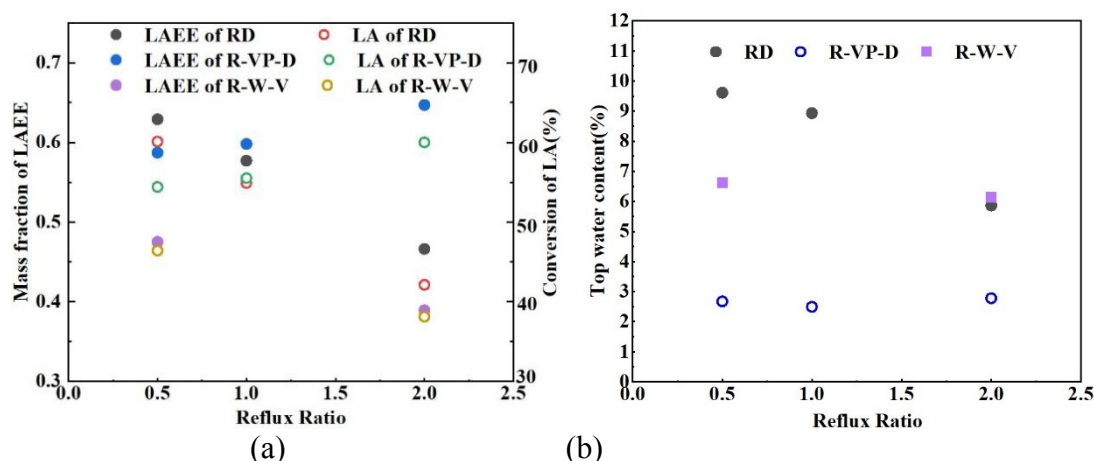| Exptl 9 | trace | 93.149 | trace | 6.851 | 47.631 | 1.293 | 50.483 | 0.59 | 0.477 |
| | | | | | | | | | 3 |

Abbreviations: LA, levulinic acid; LAEE, ethyl levulinate; R-VP-D, reactive-vapor permeation-distillation; R-W-V, reactive distillation without vapor permeation; RD, reactive distillation.

4.2 | Effect of RR

As shown in the Figure 12, in the R-VP-D process, as the RR increased from 0.5 to 2, the mass fraction of LAEE had a rise from 58.681% to 64.712%, and the conversion of LA rose to 0.6 from 0.544. Meanwhile the water content in the top of column were 2.671%, 2.493%, and 2.776% as the RR were 0.5, 1 and 2, respectively. Compared to the R-W-V process, the LA conversion of R-VP-D process had a rise up to 21.1% when the RR was 2, and 8% when the RR was 0.5; the water content in the top of R-VP-D column had reduced by 3.945% when the RR was 0.5, and 3.350% when the RR was 2. Compared to the RD process, a growing trend was observed in the R-VP-D process with RR rising from 0.5 to 2, which was completely different with the trend of RD process. The conversion of LA in the R-VP-D process was 0.6 when the RR was 2, higher than 0.421 in the RD process, and a 5.7% lower when the RR was 0.5. From the aspect of water content in the top of column, the R-VP-D process was far below RD process, a reduction of 6.937%, 6.438% and 3.085% was observed as the RR was 0.5, 1, and 2, respectively.
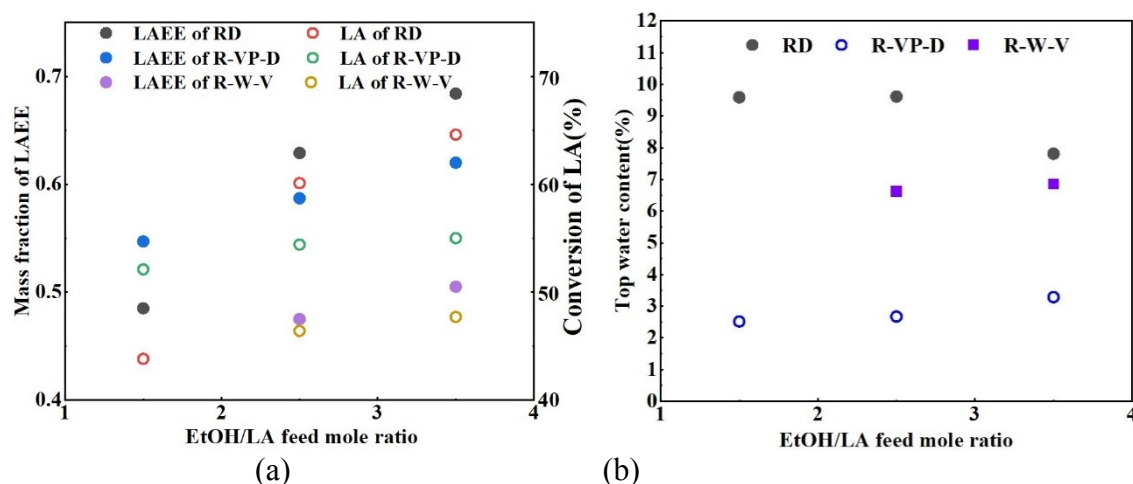
FIGURE 12 Effects of RR on purity of LAEE, conversion of LA and water content in the top of column of three different processes. (a) effects of RR on purity of LAEE, conversion of LA of three processes, (b) effects of RR on water content in the top of column of three processes. (R-VP-D experimental conditions: FMR (EtOH/LA): 2.5, total feed rate 256 kg/h, LA feeding location: Inlet point 1, EtOH feeding location: Inlet point 4, D/F: 0.40, 1atm)

Among these three processes, there were four factors that affected the synthesis of LAEE in the pilot-scale experiments, e.g. EtOH enrichment, reactants dilution effect, shorter residence time for reactants and azeotropic effect. The last three factors had hindering effects, while the first one was just the opposite. In the R-VP-D process, the introduction of VP unit between two reactive sections had a significant effect in the aspect of in situ removal of water. This effect had not only broken the EtOH and water azeotrope, but also promoted the forward progress of LAEE synthesis by the way of product removal. As shown in Figure 12b, the water content in the top of column of R-VP-D process was much less than RD and R-W-V process, which confirmed the availability of the self-designed R-VP-D column and effectiveness of the R-VP-D process. Therefore, with the increase of RR in the R-VP-D process, the azeotrope breaking effect, reaction promoting effect and EtOH enrichment were taking the dominant status gradually, which were beneficial to the converting of LA and improving of LAEE purity, thus, a completely different trend of RR on LAEE purity and LA conversion was observed in this process.

As shown in Figure 12a, compared to R-W-V process, under same residence time for reactants and same separation efficiency, the experimental results indicated that the embedding of VP unit had an obvious promoting effect on the LA conversion and LAEE purity. Compared to RD process, as R-VP-D process had a shorter residence time and lower separation efficiency on account of a shorter reactive section and less packings, the promoting effect of R-VP-D was also verified according to the partially leading experimental results.

4.3 | Effect of FMR

As shown in Figure 13, the effect of FMR was illustrated by Exptl 1, Exptl 5, Exptl 6, Exptl 7, Exptl 9, Exp 7, Exp 3, and Exp 8. Within the comparison of three different processes, a relatively gentle trend was observed and a much lower water content in the top of column was seen in the R-VP-D process. In this process, as FMR increased from 1.5 to 3.5, the conversion of LA rose from 0.521 to 0.550, and the mass fraction of LAEE had a rise up to 61.991%. The LA conversion and LAEE purity of R-VP-D process were lower than RD process when FMR were 2.5 and 3.5, but much higher in 1.5, while the R-W-V process was far behind the R-VP-D process as a maximum 7.3% difference in LA conversion was presented in the experimental results. As shown in Figure 13b, an appropriately 3% water content in the top of column was observed in R-VP-D process while there were 9% and 7% in RD and R-W-V process, which indicated a huge difference of water content in the pilot-scale column.
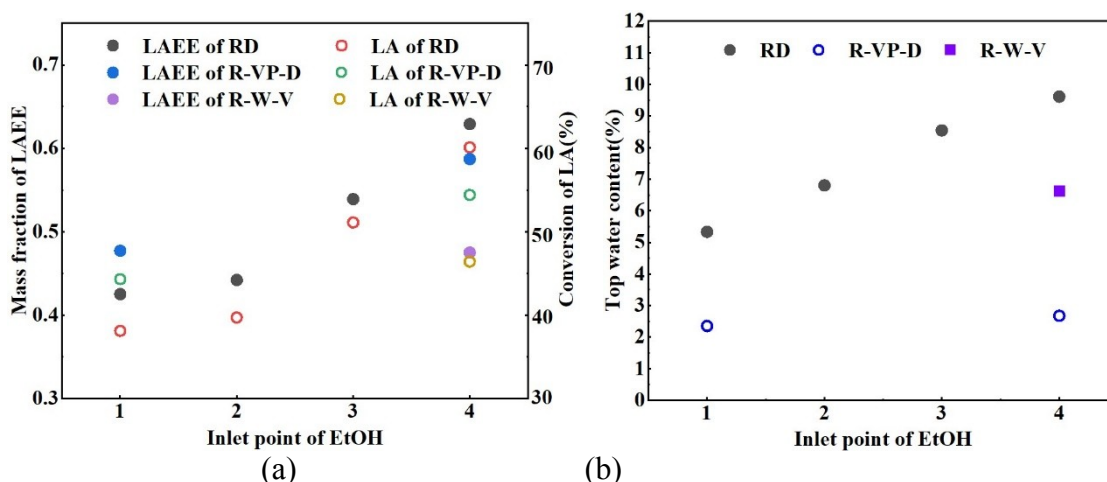
FIGURE 13 Effects of FMR on purity of LAEE, conversion of LA and water content in the top of column of three different processes. (a) effects of FMR on purity of LAEE, conversion of LA of three different processes, (b) effects of FMR on water content in the top of column of three different processes. (R-VP-D experimental conditions: RR: 0.5, LA feeding location: Inlet point 1, EtOH feeding location: Inlet point 4, 1 atm)

With an increase of FMR, the mass fraction of LA was lowered in the column as more EtOH was introduced into the column. Therefore, four critical factors were considered in the three processes, including EtOH enrichment, azeotropic effect, total residence time, and separating capacity. Obviously, among these three processes, the RD process had a higher total residence time and a better separating capacity, while the R-VP-D process had azeotrope breaking effect and in-situ product removal capacity. Thus, the R-VP-D process had a higher LA conversion than RD and R-W-V process when the FMR was 1.5, the azeotrope breaking effect and in-situ product removal capacity were dominating factors at this time. However, as the FMR was 2.5 and 3.5, the separating capacity was much more important, thus, the R-VP-D process had a lower LA conversion than RD but a higher LA conversion than R-W-V process at this time. But overall, a higher FMR brought a higher EtOH enrichment, which was crucial to the conversion of LA. Therefore, all three processes showed positive trends in the aspect of LA conversion and LAEE purity.

In usual atmospheric pressure, EtOH would form an azeotrope with water with an azeotropic temperature of 78.1°C and an azeotropic composition of 95.6 wt.% EtOH and 4.4 wt. % water. In RD, R-VP-D and R-W-V processes, the pressure of entire column was close to atmospheric pressure, and the water content in the top of column of RD and R-W-V process was higher than 4.4 wt.%, while the R-VP-D process was around 3 wt.%. This was a further evidence of the superiority of dehydration effect in R-VP-D process. In addition, under a small membrane area of 213.52 cm^2, the water content in the top of column was stable with the increment of FMR. This indicated the good dewaterability and treatment capacity of self-designed VP unit, which reviewed its greater efficiency and cost saving in the industrial scale.

4.4 | Effect of feeding position

Figure 14 showed the effect of the EtOH feed-in position on the conversion of LA, the purity of LAEE and the water content in the top of column. Among these three processes, all four inlet points had been investigated which illustrated by Exp 3, Exp 4, Exp 5 and Exp 6 in RD process, while only inlet point 1 and inlet point 4 were conducted in R-VP-D process presented by Exptl 1 and Exptl 4, and inlet point 4 was the only one performed in R-W-V process illustrated by Exptl 7. In R-VP-D process, as could be seen in Figure 14a, the conversion of LA increased from 0.443 to 0.600 when the EtOH feed position changed from inlet point 1 to inlet point 4, similarly, the mass fraction of LAEE increased from 47.710 to 64.712 wt.% as the feeding position changed.

FIGURE 14 Effects of EtOH feeding location on purity of LAEE, conversion of LA and water content in the top of column of three different processes. (a) effects of EtOH feeding location on purity of LAEE, conversion of LA and water content in the top of column of three different processes, (b) effects of EtOH feeding location on water content in the top of column of three different processes. (R-VP-D experimental conditions: RR: 0.5, FMR (EtOH/LA): 2.5, total feed rate: 256 kg/h, LA feeding location: Inlet point 1, D/F: 0.40, 1 atm)

The feeding position has a prominent influence on the concentration distribution in the column. As the EtOH was the light component, it would be vaporized immediately after feeding into the column. The reaction could only occur in the reactive section above the inlet point of EtOH. In the R-VP-D process, as shown in the Figure 14, feeding below the membrane (Inlet point 4) was obviously better than feeding above the membrane (Inlet point 1). This was not only owing to a longer contacting time of LA and EtOH, but also the longer residence time of EtOH. The water content in the top of column shown in Figure 14b indicated that VP unit still worked as EtOH fed above the membrane, which indicated multiple feeding modes were feasible in R-VP-D process.

5 | CONCLUSION

R-VP-D by embedding a hollow fiber NaA zeolite membrane module in reactive distillation column was proposed in this work for LAEE production from esterification of LA and EtOH.

Self-designed R-VP-D column which integrated separation, reaction and dehydration into one single unit had been applied and validated experimentally. The synthesis of LAEE via RD was also studied for comparison. Eight RD experiments were performed to analyze the effect of critical parameters, RR, FMR and feeding position of EtOH. Within the experimental investigation, an optimal RR of 0.5, inlet point 1 of LA, inlet point 4 of LAEE and FMR of 3.5 was obtained to get the maximum LA conversion of 0.646 and maximum LAEE purity of 68.350 wt.%.

Several self-designed apparatuses including MMIC, MSS and R-VP-D column were introduced and the feasibility of them had been verified in this article. Six R-VP-D experiments and three R-W-V experiments were conducted to illustrate the effect of RR, FMR and feeding position of EtOH on LAEE purity, LA conversion and water content in the top of column. In addition, a comparison of RD, R-VP-D, and R-W-V process was performed. For the RR of 2, the feed mole ratio of 3.5, the LA feeding position of Inlet1, and the EtOH feeding position of Inlet4, the R-VP-D process could achieve a relatively good result which had LA conversion of 0.600 and LAEE purity of 64.712 wt.%.

A maximum 21.9% higher than R-W-V process in LA conversion and a maximum 25.792% higher than R-W-V process in LAEE purity were observed in R-VP-D experiment, where up to 53.634% of products water could be removed from VP module. This indicated the significant effect of R-VP-D process in azeotrope overcoming and reaction promoting with a only small membrane area of 213.52 cm^2 inside the RD column. The investigation raised a new concept in the aspect of coupling membrane and RD, and the improved column setup would be useful for equilibrium-limited reactions on an industrial-scale.

ACKNOWLEDGMENTS

REFERENCES

1. Joshi H, Moser BR, Toler J, Smith WF, Walker T. Ethyl levulinate: a potential bio-based diluent for biodiesel which improves cold flow properties. *Biomass Bioenergy*. 2011;35(7):3262-3266.

2. Resk AJ, Peereboom L, Kolah AK, Miller DJ, Lira CT. Phase equilibria in systems with levulinic acid and ethyl levulinate. *J Chem Eng Data*. 2014;59(4):1062-1068.

3. Huber GW, Iborra S, Corma A. Synthesis of transportation fuels from biomass: chemistry, catalysts, and engineering. *Chem Rev*. Sep 2006;106(9):4044-4098.

4. Kiss AA, Jobson M, Gao X. Reactive distillation: stepping up to the next level of process intensification. *Ind Eng Chem Res*. 2018;58(15):5909-5918.

5. Taylor R, Krishna R. Modelling reactive distillation. *Chem Eng Sci*. 2000/11/01 2000;55(22):5183-5229.

6. Buchaly C, Kreis P, Górak A. Hybrid separation processes—combination of reactive distillation with membrane separation. *Chem Eng Process*. 2007;46(9):790-799.

7. Lin Y-D, Chen J-H, Cheng J-K, Huang H-P, Yu C-C. Process alternatives for methyl acetate conversion using reactive distillation. 1. Hydrolysis. *Chem Eng Sci*. 2008;63(6):1668-1682.

8. da Silva Nde L, Santander CM, Batistella CB, Filho RM, Maciel MR. Biodiesel production from integration between reaction and separation system: reactive distillation process. *Appl Biochem Biotechnol*. May 2010;161(1-8):245-254.

9. Kiss AA, Bildea CS. A review of biodiesel production by integrated reactive separation technologies. *J Chem Technol Biotechnol*. 2012;87(7):861-879.

10. Novita FJ, Lee H-Y, Lee M. Self-heat recuperative dividing wall column for enhancing the

energy efficiency of the reactive distillation process in the formic acid production process. *Chem Eng Process*. 2015;97:144-152.

11. Nagai K. 2.10 - Fundamentals and perspectives for pervaporation. In: Drioli E, Giorno L, eds. *Comprehensive Membrane Science and Engineering*. Oxford: Elsevier; 2010:243-271.

12. Luis P, Amelio A, Vreysen S, Calabro V, Van der Bruggen B. Simulation and environmental evaluation of process design: distillation vs. hybrid distillation–pervaporation for methanol/tetrahydrofuran separation. *Appl Energy*. 2014;113:565-575.

13. Harvianto GR, Ahmad F, Nhien LC, Lee M. Vapor permeation–distillation hybrid processes for cost-effective isopropanol dehydration: modeling, simulation and optimization. *J Membr Sci*. 2016;497:108-119.

14. Li H, Guo C, Guo H, Yu C, Li X, Gao X. Methodology for design of vapor permeation membrane-assisted distillation processes for aqueous azeotrope dehydration. *J Membr Sci*. 2019;579:318-328.

15. Fontalvo J, Cuellar P, Timmer JMK, Vorstman MAG, Wijers JG, Keurentjes JTF. Comparing Pervaporation and Vapor Permeation Hybrid Distillation Processes. *Ind Eng Chem Res*. 2005;44(14):5259-5266.

16. Roth T, Kreis P, Górak A. Process analysis and optimisation of hybrid processes for the dehydration of ethanol. *Chem Eng Res Des*. 2013;91(7):1171-1185.

17. Holtbruegge J, Wierschem M, Lutze P. Synthesis of dimethyl carbonate and propylene glycol in a membrane-assisted reactive distillation process: pilot-scale experiments, modeling and process analysis. *Chem Eng Process*. 2014;84:54-70.

18. Novita FJ, Lee H-Y, Lee M. Reactive distillation with pervaporation hybrid configuration for enhanced ethyl levulinate production. *Chem Eng Sci*. 2018;190:297-311.

19. Steinigeweg S, Gmehling J. Transesterification processes by combination of reactive distillation and pervaporation. *Chem Eng Process*. 2004;43(3):447-456.

20. Liu D, Zhang Y, Jiang J, Wang X, Zhang C, Gu X. High-performance NaA zeolite

membranes supported on four-channel ceramic hollow fibers for ethanol dehydration. *RSC Adv*. 2015;5(116):95866-95871.

21. Ji M, Gao X, Wang X, Zhang Y, Jiang J, Gu X. An ensemble synthesis strategy for fabrication of hollow fiber T-type zeolite membrane modules. *J Membr Sci*. 2018;563:460-469.

22. Gao X, Li X, Zhang R, Li H. Pressure drop models of seepage catalytic packing internal for catalytic distillation column. *Ind Eng Chem Res*. 2012;51(21):7447-7452.

23. Li X, Zhang H, Gao X, Zhang R, Li H. Hydrodynamic simulations of seepage catalytic packing internal for catalytic distillation column. *Ind Eng Chem Res*. 2012;51(43):14236-14246.

24. Gao X, Wang F, Zhang R, Li H, Li X. Liquid flow behavior of a seepage catalytic packing internal for catalytic distillation column. *Ind Eng Chem Res*. 2014;53(32):12793-12801.

25. Richter H, Voigt I, Kühnert J-T. Dewatering of ethanol by pervaporation and vapour permeation with industrial scale NaA-membranes. *Desalination*. 2006;199(1-3):92-93.

26. Wang X, Jiang J, Liu D, Xue Y, Zhang C, Gu X. Evaluation of hollow fiber T-type zeolite membrane modules for ethanol dehydration. *Chin J Chem Eng*. 2017;25(5):581-586.

27. Gao X, Wang S, Wang J, Xu S, Gu X. The study on the coupled process of column distillation and vapor permeation by NaA zeolite membrane for ethanol dehydration. *Chem Eng Res Des*. 2019;150:246-253.

28. Wang J, Gao X, Ji G, Gu X. CFD simulation of hollow fiber supported NaA zeolite membrane modules. *Sep Purif Technol*. 2019;213:1-10.